The Ellsworth Subglacial Highlands: Inception and retreat of the West Antarctic Ice Sheet

Neil Ross[1,†], Tom A. Jordan[2], Robert G. Bingham[3], Hugh F.J. Corr[2], Fausto Ferraccioli[2], Anne Le Brocq[4], David M. Rippin[5], Andrew P. Wright[4], and Martin J. Siegert[6]

[1]*School of Geography, Politics and Sociology, Newcastle University, Newcastle upon Tyne, NE1 7RU, UK*
[2]*British Antarctic Survey, Cambridge CB3 0ET, UK*
[3]*School of Geosciences, University of Edinburgh, Edinburgh EH8 9XP, UK*
[4]*School of Geography, University of Exeter, Exeter EX4 4RJ, UK*
[5]*Environment Department, University of York, York YO10 5DD, UK*
[6]*Bristol Glaciology Centre, School of Geographical Sciences, University of Bristol, Bristol BS8 1SS, UK*

ABSTRACT

Antarctic subglacial highlands are where the Antarctic ice sheets first developed and the "pinning points" where retreat phases of the marine-based sectors of the ice sheet are impeded. Due to low ice velocities and limited present-day change in the ice-sheet interior, West Antarctic subglacial highlands have been overlooked for detailed study. These regions have considerable potential, however, for establishing the locations from which the West Antarctic Ice Sheet originated and grew, and its likely response to warming climates. Here, we characterize the subglacial morphology of the Ellsworth Subglacial Highlands, West Antarctica, from ground-based and aerogeophysical radio-echo sounding (RES) surveys and the Moderate-Resolution Imaging Spectroradiometer (MODIS) Mosaic of Antarctica. We document well-preserved classic landforms associated with restricted, dynamic, marine-proximal alpine glaciation, with hanging tributary valleys feeding a significant overdeepened trough (the Ellsworth Trough) cut by valley (tidewater) glaciers. Fjord-mouth threshold bars down-ice of two overdeepenings define both the northwest and southeast termini of paleo-outlet glaciers, which cut and occupied the Ellsworth Trough. Satellite imagery reveals numerous other glaciated valleys, terminating at the edge of deep former marine basins (e.g., Bentley Subglacial Trench), throughout the Ellsworth Subglacial Highlands. These geomorphic data can be used to reconstruct the glaciology of the ice masses that formed the proto–West Antarctic Ice Sheet. The landscape predates the present ice sheet and was formed by a small dynamic ice field(s), similar to those of the present-day Antarctic Peninsula, at times when the marine sections of the West Antarctic Ice Sheet were absent. The Ellsworth Subglacial Highlands represent a major seeding center of the paleo–West Antarctic Ice Sheet, and its margins represent the pinning point at which future retreat of the marine-based West Antarctic Ice Sheet would be arrested.

INTRODUCTION

The West Antarctic Ice Sheet rests largely on a bed several hundred meters below sea level. As a marine-based ice sheet, it may be inherently unstable due to its sensitivity to ocean temperatures and upstream deepening of its bed in a number of key areas (Weertman, 1974; Bamber et al., 2009a; Joughin and Alley, 2011). However, despite it being critical to our evaluation of West Antarctic Ice Sheet inception, stability, and the likelihood of future sea-level change from ice-sheet loss (Bentley, 2010), the glacial history of West Antarctica is not well constrained.

The recognition that the subglacial highlands of East Antarctica acted as critical nucleation sites for the East Antarctic Ice Sheet has driven much recent research (e.g., Bo et al., 2009; Bell et al., 2011; Ferraccioli et al, 2011). In comparison, however, the subglacial upland areas of the West Antarctic Ice Sheet have been little investigated. Two dominant upland regions, which may be instrumental in the growth and decay of the ice sheet, exist beneath the West Antarctic Ice Sheet: the Ellsworth Subglacial Highlands, and the coastal mountain ranges of Marie Byrd Land, centered around the Executive Committee Range (Fig. 1A). Bentley et al. (1960) hypothesized that these uplands were the main seeding grounds of West Antarctic Ice Sheet growth, while Bamber et al. (2009) hypothesized them as pinning points of a retreating ice sheet. Testing these hypotheses requires evidence of former ice dynamics. Several investigations in East Antarctica have demonstrated the utility of radio-echo sounding (RES) in mapping ancient glacial geomorphic features from which ice-sheet reconstructions can be based (Bo et al., 2009; Young et al., 2011). Here, we present geophysical data on the morphology of the Ellsworth Subglacial Highlands, gained during three seasons of ground-based and airborne RES measurements around Ellsworth Subglacial Lake (Woodward et al., 2010) and over the Institute and Möller ice streams (see Fig. 1; Ross et al., 2012). These surveys have revealed a deep (>2000 m below sea level [bsl]), broad (up to 25 km across), and >300-km-long subglacial trough, named the Ellsworth Trough, which dissects the Ellsworth Subglacial Highlands northwest to southeast (Fig. 2). Aligned roughly parallel to linear topographic trends in the Ellsworth Mountains, and bounded on both sides by rugged mountainous subglacial topography, the Ellsworth Trough is one of a series of NW-SE–trending subglacial valleys extending from the core of the Ellsworth Subglacial Highlands into the Bentley Subglacial Trench (Fig. 1), several of which contain subglacial lakes (Vaughan et al., 2006, 2007). The Ellsworth Trough lies roughly orthogonal to the Amundsen-Weddell ice divide (Ross et al., 2011), currently contains Ellsworth Subglacial Lake (Woodward et al., 2010; Siegert et al., 2012), and hosts an enhanced-flow tributary of Institute Ice stream (Joughin et al., 2006; Rignot et al., 2011), which connects to the deep marine basin (the "Robin Subglacial Basin") that underlies the coastal parts of the Institute Ice stream and Möller Ice stream (Ross et al., 2012).

[†]E-mail: neil.ross@ncl.ac.uk

GSA Bulletin; January/February 2014; v. 126; no. 1/2; p. 3–15; doi: 10.1130/B30794.1; 9 figures.

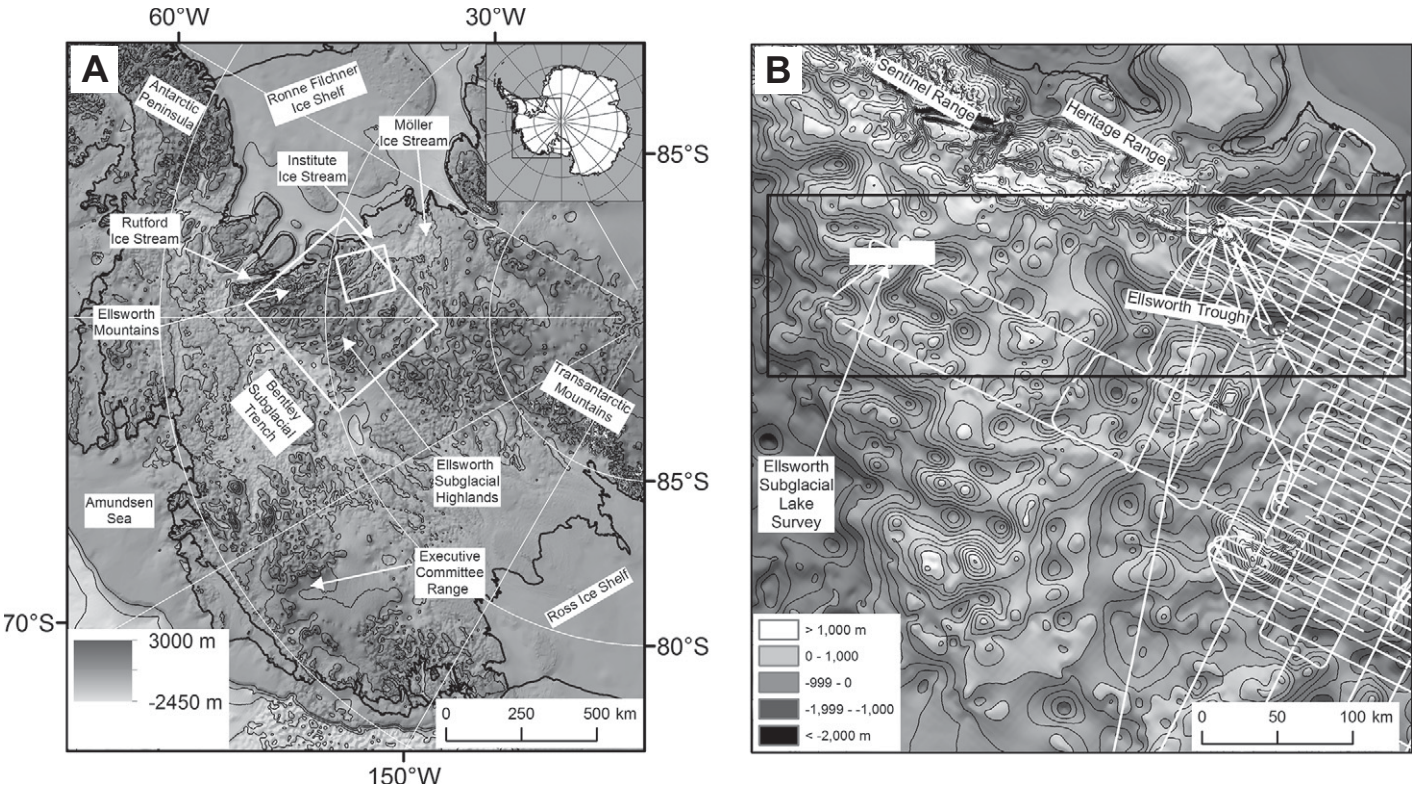

Figure 1. (A) Subglacial topography of West Antarctica (BEDMAP2) (m WGS84) (Fretwell et al, 2013), showing areas of Figures 1B, 6A–6C, 7A (large white box), and 3C (small white box). Inset shows location of study area. Thin black lines are bed topography contours at 1000 m intervals. (B) Subglacial topography of the Ellsworth Subglacial Highlands (BEDMAP2) (m WGS84) (Fretwell et al., 2013). Filled white polygons represent areas of exposed bedrock of the Sentinel and Heritage Ranges (from SCAR Antarctic Digital Database [ADD] (http://www.add.scar.org/terms.isp). The white in-filled box delimits the area of the 2007–2009 ground-based RES survey of Ellsworth Subglacial Lake (Fig. 3A). Thick white lines show bed elevation measurements made during the 2010–2011 aerogeophysical survey of the Institute and Möller ice streams. Location of Figure 2 (large black rectangle) is shown. Thin black lines are bed topography contours at 250 m intervals.

In this paper, we first describe and interpret (1) high-resolution ground-based radar data acquired over the northwestern parts of the Ellsworth Trough; and (2) airborne radar data acquired over the southeastern parts of the Ellsworth Trough. We then combine the bed topographic data with ice-surface remote-sensing data to place our interpretation of these data into the broader context of the Ellsworth Subglacial Highlands and West Antarctica.

METHODS

Radio-Echo Sounding, the Northwestern Ellsworth Trough

Ground-based RES data were acquired over and around the Ellsworth Trough during the 2007–2008 and 2008–2009 Antarctic field seasons (Fig. 1B; Siegert et al., 2012). Data were acquired with the low-frequency (~2 MHz) DELORES (DEep-LOok Radio Echo Sounder) radar (further details of the system are provided in King, 2009). Acquisition was undertaken using half-dipole lengths of 40 m with the system towed behind a snowmobile traveling at ~12 km h^{-1}. Measurements were stacked 1000 times, giving along-track measurements (traces) every 2–5 m. Roving global positioning system (GPS) data, to locate the *x*-*y*-*z* positions of individual radar traces, were acquired using a GPS antenna secured on the radar receiver sledge. Differential GPS processing used daily precise point positioning (PPP)–processed positions of a GPS receiver located over the center of Ellsworth Subglacial Lake as the fixed reference station. Roving data were corrected for the ~90 m offset between the GPS receiver and the midpoint between the radar transmitter and receiver. Radar data processing, undertaken using REFLEXW processing

Figure 2 (*on following page*). (A) Moderate-Resolution Imaging Spectroradiometer (MODIS) Mosaic of Antarctica (MOA) digital image mosaic of the surface morphology of the Antarctic ice sheet (Haran, 2005; Scambos et al., 2007) over and around the Ellsworth Trough (ET) (see Fig. 1B for location). Small white box (in A–C) delimits area of ground-based survey around Ellsworth Subglacial Lake. Filled white polygons (in A–D) represent subaerially exposed bedrock (from SCAR Antarctic Digital Database [ADD] (http://www.add.scar.org/terms.isp). (B) Profile curvature analysis of MODIS MOA data around the Ellsworth Trough. Cells with curvature <–0.05 and >0.05 are colored black; cells with curvature between –0.05 and 0.05 are colored light gray. (C) Ice-sheet surface velocity (Rignot et al., 2011) superimposed on profile curvature map. Color scale of velocity data is on a log scale and is saturated at 130 m yr^{-1}. Black contours are in 25 m yr^{-1} intervals. (D) Bedrock elevation (m WGS84) from surveys of Ellsworth Subglacial Lake and Institute and Möller ice streams superimposed on map of profile curvature.

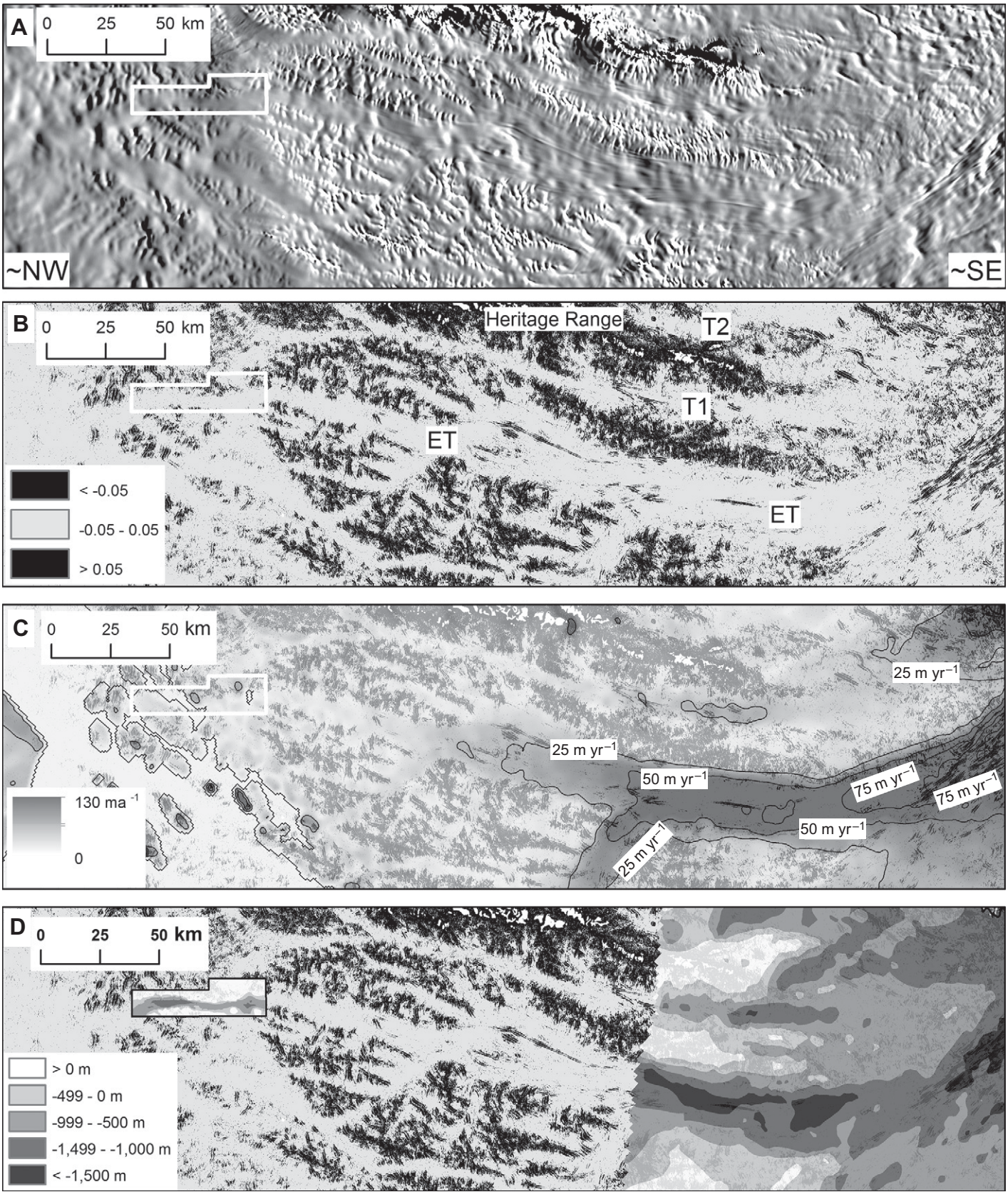

Figure 2.

software, involved: (1) band-pass frequency filtering; (2) gain correction; and (3) migration. The peak of the first "bed" return of each trace was picked, and ice thickness was calculated from the two-way traveltime of the bed pick using a velocity of 0.168 m ns^{-1}. No firn correction was applied. Ice thickness was subtracted from the GPS-derived ice-surface elevation of each trace to establish bed elevations relative to the WGS84 ellipsoid. DELORES-derived bed elevations were combined with contours from a seismic-reflection–derived grid of the floor of Ellsworth Subglacial Lake (Woodward et al., 2010) and gridded, using the ARCGIS "Topo to Raster" interpolation function, to produce a combined digital elevation model of the subice and sublake topography.

Radio-Echo Sounding, the Southeastern Ellsworth Trough

Approximately 25,000 line km of aerogeophysical survey data were obtained over Institute and Möller ice streams during the 2010–2011 Antarctic field season (Fig. 1B; Ross et al., 2012). Data were acquired using the British Antarctic Survey (BAS) airborne radar system installed on a ski-equipped Twin Otter aircraft. Full details of data acquisition and processing have been reported previously (e.g., Corr et al., 2007; Ross et al., 2012; Karlsson et al., 2012), but a brief summary is provided here. The ice-sounding radar is a coherent system with a frequency of 150 MHz. Aircraft position and elevation were obtained from onboard differential GPS, corrected using GPS base stations from two remote field camps. The ice-sheet surface elevation was established from radar or laser altimeter terrain-clearance measurements. Processing and the semi-automated picking of the radar data were undertaken using PROMAX processing software, with Doppler processing used to migrate radar-scattering hyperbolae in the along-track direction. Ice thickness, at an along-track interval of ~10 m, was calculated from the two-way traveltime of the bed pick using a velocity of 0.168 m ns^{-1} and a firn layer correction of 10 m. Ice thickness was subtracted from the ice-surface elevation of each trace to establish bed elevations relative to the WGS84 ellipsoid. Bed elevations were then gridded, using the ArcGIS Natural Neighbor interpolation algorithm, to produce a digital elevation model of the subglacial topography.

Satellite Imagery

The Moderate-Resolution Imaging Spectroradiometer (MODIS) Mosaic of Antarctica (MOA) (Scambos et al., 2007) is a digital image mosaic of the surface morphology of the Antarctic ice sheet, derived from red-light and infrared imagery of the Antarctic continent. This mosaic has considerable potential for shedding light on ice-sheet flow and sub-ice landforms and structures. We investigated the MODIS MOA imagery (Fig. 2A) to assess its ability to reflect underlying subglacial topography. Basal morphology influences ice-surface elevation, and hence ice-sheet surface imagery, due to the viscous response of ice as it flows over subglacial relief. Increasing ice thickness acts to damp the response to subglacial topography, so regions of thin ice within subglacial highlands are associated with more rugged surface topography and variable surface imagery compared with areas of thicker ice. Earlier studies have demonstrated the effectiveness of applying surface-curvature analysis to characterize these trends over regions of the ice sheet (Rémy and Minster, 1997; Le Brocq et al., 2008). Hence, we assessed the variability of the MODIS imagery to map the Ellsworth Subglacial Highlands by applying the ArcGIS Raster Curvature function to the 125-m-resolution MOA surface morphology image map (Haran et al., 2005). The Raster Curvature function calculates the second derivative (i.e., the slope of the slope) of a surface (in this case, the MODIS MOA image) on a cell-by-cell basis (Kimerling et al., 2011). The first derivative converts regional trends in the image to a simple level offset, while the second derivative converts all level offsets to zero. Areas with the most variable surface imagery, and likely thin ice, are therefore revealed as regions with high or low second derivative values (>0.05, or <–0.05). Three outputs are generated by the Raster Curvature function: (1) profile curvature—the curvature of the surface parallel to the direction of the maximum slope; (2) plan curvature—the curvature of the surface perpendicular to the direction of the maximum slope; and (3) curvature—the overall curvature of a surface, i.e., the combination of the profile and plan curvature. For our data, the profile curvature proved to be the most useful for investigating our area of interest (i.e., the Ellsworth Subglacial Highlands). For profile curvature, at any given cell location, a negative value indicates that the surface is upwardly convex at that point, a positive value indicates the surface to be upwardly concave, and a value of zero indicates a linear surface.

RESULTS

Radio-Echo Sounding of the Ellsworth Trough

The geomorphology of the Ellsworth Trough and its surrounding area is diagnostic of a well-developed glaciated valley network. This section describes the geomorphology of the Ellsworth Trough from RES data acquired over the northwestern (high-resolution ground-based data) and southeastern (airborne data) ends of the trough (Figs. 2 and 3).

The northwestern sector of the Ellsworth Trough (Figs. 1 and 2) has a relief exceeding 2500 m, contains ice in excess of 3200 m thick, is up to 7 km wide, and is classically U-shaped (Fig. 3A). Toward the present-day Amundsen-Weddell ice divide, in the south-eastern parts of the ground-based survey, the base of the Ellsworth Trough is characterized by subdued relief (800–1000 m bsl) and valley-floor morphology for nearly 30 km (Fig. 3B).

Approximately 6 km up-ice of the Ellsworth Subglacial Lake, the trough floor begins to deepen, with a steep slope down to the lake margin at ~1200 m bsl. Ellsworth Subglacial Lake lies within the Ellsworth Trough in an ~15–20-km-long overdeepened basin. Seismic-reflection data (Woodward et al., 2010) show that the lake floor reaches a minimum elevation of 1393 ± 10 m bsl, ~400 m below the average elevation of the upper trough (Figs. 3A and 3B). The rock-sediment interface of the overdeepening must lie below the minimum elevation of the lake bed observed in the seismic data, however, because acoustic impedance analysis suggests that the lake bed is a water-sediment boundary (Woodward et al., 2010; Siegert et al., 2012). Down-ice, towards the northwest, the trough bed (i.e., the base of the lake) rises sharply to a prominent ridge, which currently impounds Ellsworth Subglacial Lake. Roughly orthogonal to present-day ice flow, the ridge (Ellsworth Subglacial Lake Ridge (ESLR)), ~1.5 km wide, lies at an oblique angle across the entire width (~7 km) of the valley. At an elevation of ~835 m bsl, the ridge crest is ~200 m above the elevation of the down-ice lake margin and at least 550 m above the base of the overdeepening (Fig. 3B). Immediately down-ice of the ridge, there is a narrow linear depression (5 km × 0.75 km) (Figs. 3A and 3B), oriented parallel to the ridge, beyond which the bed elevation rises (Fig. 3B). The Ellsworth Trough broadens down-ice of the lake and the impounding ridge (Fig. 3A).

Prominent steep-sided bedrock walls confine both sides of the northwestern parts of the Ellsworth Trough along the majority of its length (Fig. 3A). These valley sidewalls contain a number of deep tributary "hanging" valleys, oriented roughly orthogonal to the main trough axis and present-day ice flow. The hanging valleys have a smooth concave, U-shaped cross-profile (Fig. 4). They are significant features; the largest is ~3 km across (ridge-crest to ridge-crest) and ~1 km deep, with a valley floor perched >1 km above the floor of the Ellsworth Trough, at an

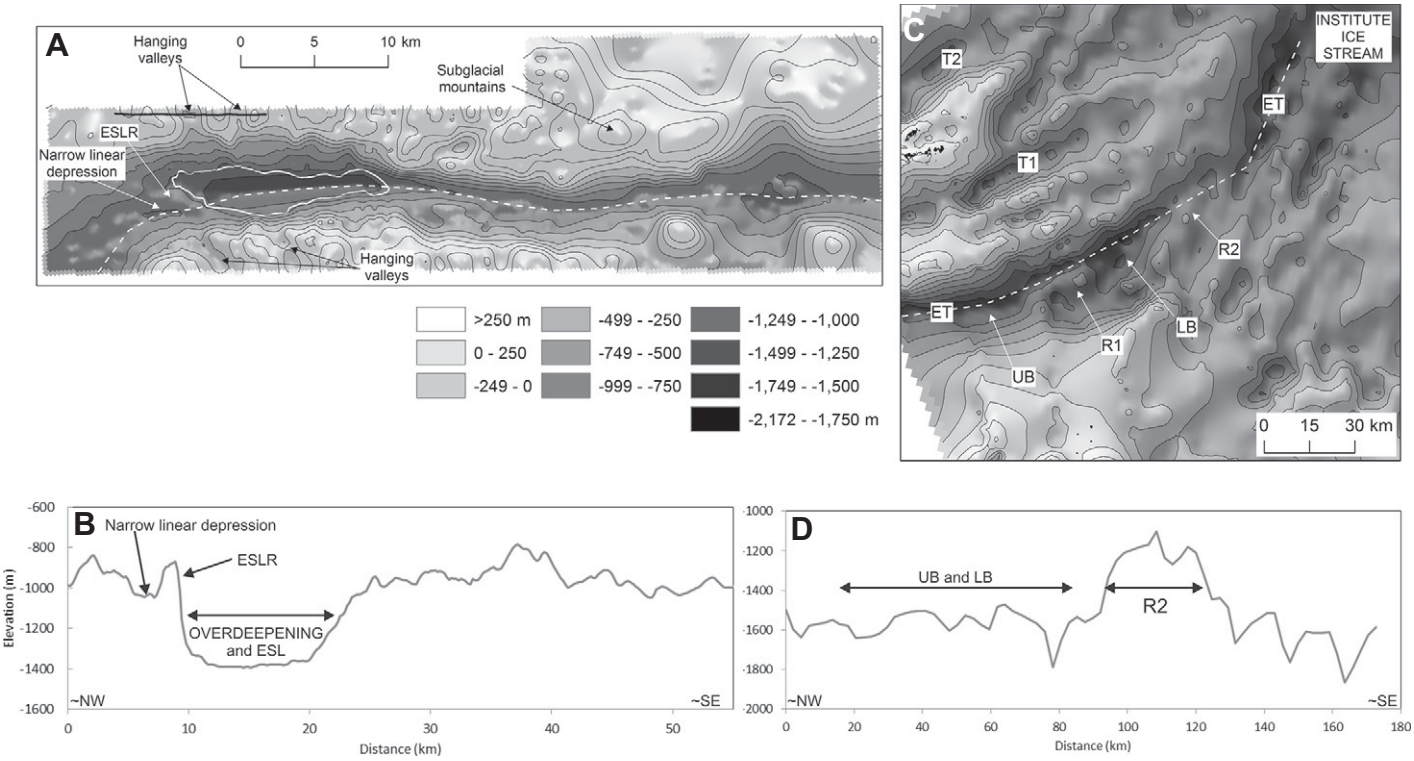

Figure 3. (A) Subglacial topography of the northwestern parts of the Ellsworth Trough from DELORES ground-based radio-echo sounding and seismic reflection data. Contours are in 250 m intervals. White dashed line shows location of profile in B. Black line is location of Figure 4. ESLR—Ellsworth Subglacial Lake Ridge. (B) Long-axis profile of the subglacial topography of the northwestern parts of the Ellsworth Trough, in the vicinity of Ellsworth Subglacial Lake (ESL). (C) Subglacial topography of the southeastern end of the Ellsworth Trough (ET) from airborne radio-echo sounding. Contours are in 250 m intervals. The three major valleys extending from the Ellsworth Subglacial Highlands are labeled Ellsworth Trough, T1, and T2; the two subbasins of the Ellsworth Trough are labeled UB (upper basin) and LB (lower basin). White dashed line shows location of profile in D. (D) Long-axis profile of the subglacial topography of the southeastern parts of the Ellsworth Trough.

elevation of –100–0 m bsl. The three-dimensional form of these features, suggested by the gridded bed (Fig. 3A), is not an artifact of the interpolation procedure; in many cases, individual hanging valleys are either observed in more than one parallel survey line, or orthogonal survey lines intersect above the valley axis. Most of the hanging valleys aligning the Ellsworth Trough are confluent with, or just up-valley of, the main trough overdeepening that contains Ellsworth Subglacial Lake (Fig. 3A), consistent with glaciological theory and observations (Linton, 1963; Crabtree, 1981).

Aerogeophysical data acquired over the upper catchments of Institute and Möller ice streams have also allowed us to characterize the subglacial topography of the southeastern end of the Ellsworth Trough (Figs. 1 and 2). The Ellsworth Trough is one of three major valleys (Ellsworth Trough, trough 1 [T1], and trough 2 [T2] [Horseshoe Valley]; Fig. 3C) that enter the deep subglacial basin beneath Institute ice stream (Ross et al., 2012). The Ellsworth Trough is the widest and deepest of these valleys, however, at >30 km across, and, at the deepest point that we were able to measure, >2 km deep. Ice thickness over some parts of the southeastern Ellsworth Trough exceeds 3000 m. Like the northwestern end of the trough, mountainous topography lines both sides of the southeastern Ellsworth Trough. Such topography is most prominent to the northeast of the trough (between ET and T1), where an elongated ridge is found, 0–500 m above sea level, and characterized by numerous hanging valleys, mountain peaks, and ridges. In some of the deepest parts of the trough, the higher-frequency airborne radar was unable to image the trough floor, although the overall form of the southeastern Ellsworth Trough is generally well characterized. Our data suggest that the valley floor of the southeastern Ellsworth Trough consists of a series of basins separated by rock bars (Fig. 3C). An upper basin (UB) (60 km long and 1500–1700 m below sea level) is separated from a lower basin (LB) (30 km long and 1500–2100 m below sea level) by a prominent, but dissected, ridge (R1) 1200–1500 m below sea level. The lower basin terminates at a broad (25 km) area of higher relief (R2) (1000–1500 below sea level), which lies across the entire width (~35 km) of the valley (Figs. 3C and 3D). Like the ridge that terminates the overdeepening associated with Ellsworth Subglacial Lake in the northwestern Ellsworth Trough (Ellsworth Subglacial Lake Ridge), R2 is located where the trough broadens down-ice as it enters a deep subglacial basin. The southeastern sector of the Ellsworth Trough is an enhanced-flow tributary of Institute ice stream. Present-day ice flow through the southeastern parts of the Ellsworth Trough, over UB, R1, LB, and R2, ranges between 50 and 75 m yr^{-1} (Rignot et al., 2011) (Fig. 2C). Down-ice of R2, the basal topography falls away again (>2000 m below sea level; Figs. 3C and 3D), and ice velocity increases markedly, exceeding 125 m yr^{-1} 25 km down-ice of the ridge (Rignot et al., 2011).

Mapping the Ellsworth Subglacial Highlands with Satellite Imagery

In this section, we use MODIS MOA ice-surface imagery to demonstrate that the northwestern and southeastern ends of the Ellsworth Trough, as described previously, are directly

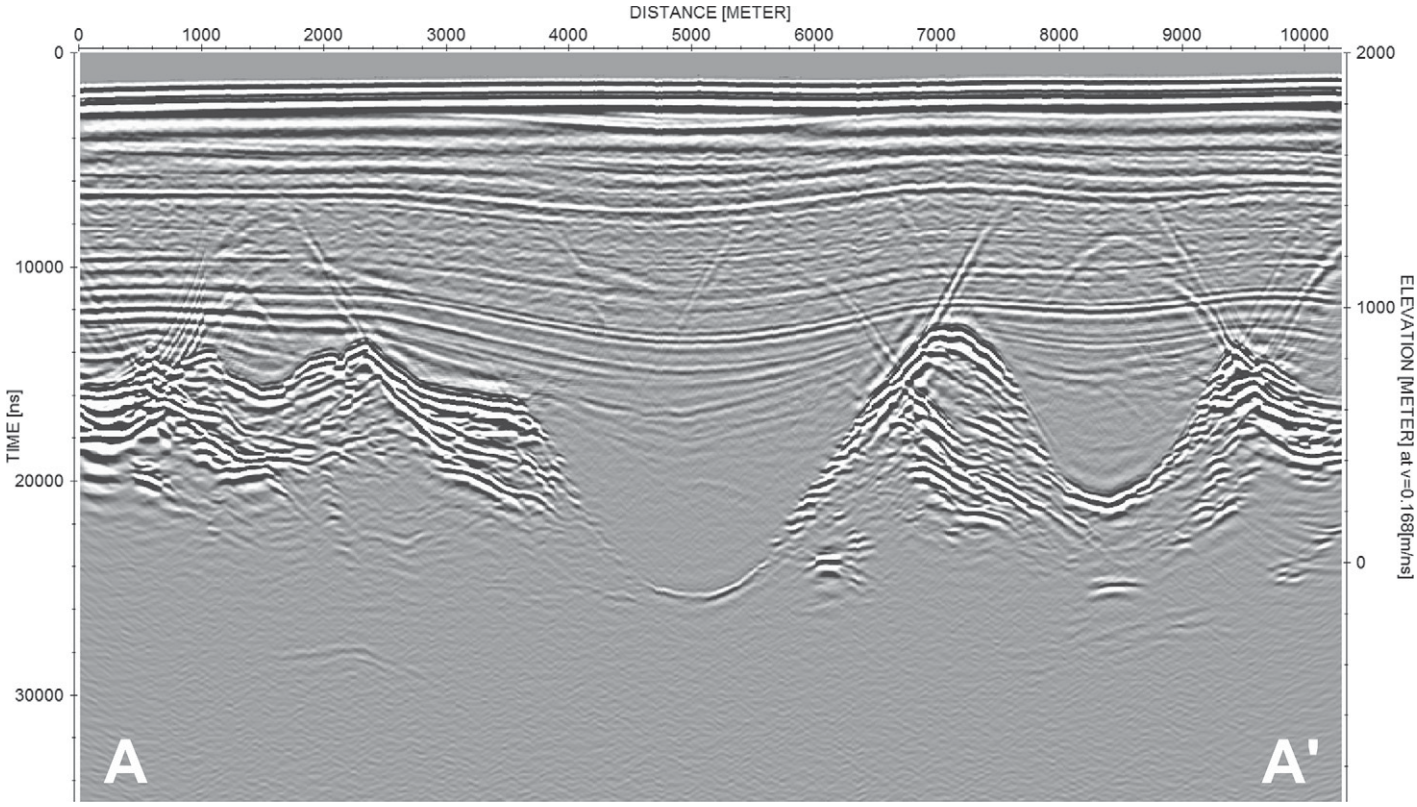

Figure 4. U-shaped hanging tributary valleys of the Ellsworth Trough. The radar survey line is located northeast of the lower parts of the Ellsworth Trough (see Figs. 3A and 5A) and runs approximately parallel to the trough and present-day ice flow (which is roughly right to left across radargram). The radargram depicts two obvious tributary valleys, the largest of which is 1 km deep by 3 km wide. The ice flow responsible for the formation of these features flowed out of the page, i.e., perpendicular to present-day ice flow.

connected as a deep subglacial valley across the entirety of the Ellsworth Subglacial Highlands mountain range. We also demonstrate that the Ellsworth Trough may only be one of several similar troughs within the Ellsworth Subglacial Highlands.

Comparing subglacial geomorphology with MODIS MOA surface imagery (as outlined in the Methods section), a striking correlation between the basal topography and the relative texture of the ice surface is apparent (Fig. 5). The deep Ellsworth Trough, as mapped by RES surveys, corresponds with a distinct "smooth" ice surface (i.e., there is little localized spatial variability in MODIS MOA ice-surface imagery) (Figs. 5A and 5B), while the surrounding subglacial mountains are associated with a discrete "rough" ice surface (i.e., there is significant and high-amplitude localized spatial variability in MODIS ice-surface imagery). We are not the first to suggest a relationship between satellite imagery of the ice sheet surface and the form of the subglacial bed (see Crabtree, 1981; Denton et al., 1992; Jezek, 1999), but our high-resolution mapping of the northwestern end of the Ellsworth Trough enables us to confirm the close relationship between the two. The contrast in texture is believed to be caused by a combination of ice flow over bedrock bumps (Gudmundsson, 2003; Smith et al., 2006) and differential surface accumulation (Welch and Jacobel, 2005) associated with marked and abrupt variations in the relief of basal topography (i.e., between deep valleys and rugged high-relief uplands). Profile curvature analysis of the MODIS MOA imagery over and around the Ellsworth Trough clearly emphasizes the major subglacial geomorphic features of interest (Fig. 5C).

The profile curvature analysis of the MODIS ice-surface imagery clearly shows that the northwestern and southeastern parts of the Ellsworth Trough are directly connected (Fig. 2), marking out the Ellsworth Trough as a glacial breach that cuts through the entire Ellsworth Subglacial Highlands. This suggestion is supported by along-track bed elevation measurements acquired by other surveys beyond those parts of the trough that we surveyed (Vaughan et al., 2006; A. Rivera personal comun., 2011); all existing evidence is consistent with a long, deep subglacial trough that breaches the mountain range.

The relationship between the high-resolution basal topography of the Ellsworth Trough and the MODIS MOA ice-surface imagery can be extrapolated to allow the geomorphology of large parts of the Ellsworth Subglacial Highlands to be inferred (Figs. 6A–6C). The correlation between the profile curvature map derived from the MODIS imagery and the bed topography is also strong in other subglacial highland areas of West Antarctica where good bed topography data exist (e.g., in parts of Marie Byrd Land; Blankenship et al., 2001), providing confidence in the use of the MODIS MOA profile curvature map as a proxy for inferring the planform of the bed topography across the entire Ellsworth Subglacial Highlands in regions where RES data are uncommon (Fig. 6C). Because the broader topography of the Ellsworth Subglacial Highlands is not known in detail, the Ellsworth Trough is currently the only subglacial valley that can be confidently proposed as a deep glacial breach through the entire range. Based on the profile curvature analysis of the MODIS MOA imagery, however, we hypothesize that several deep broad glacial troughs, many previously unmapped, lined by numerous

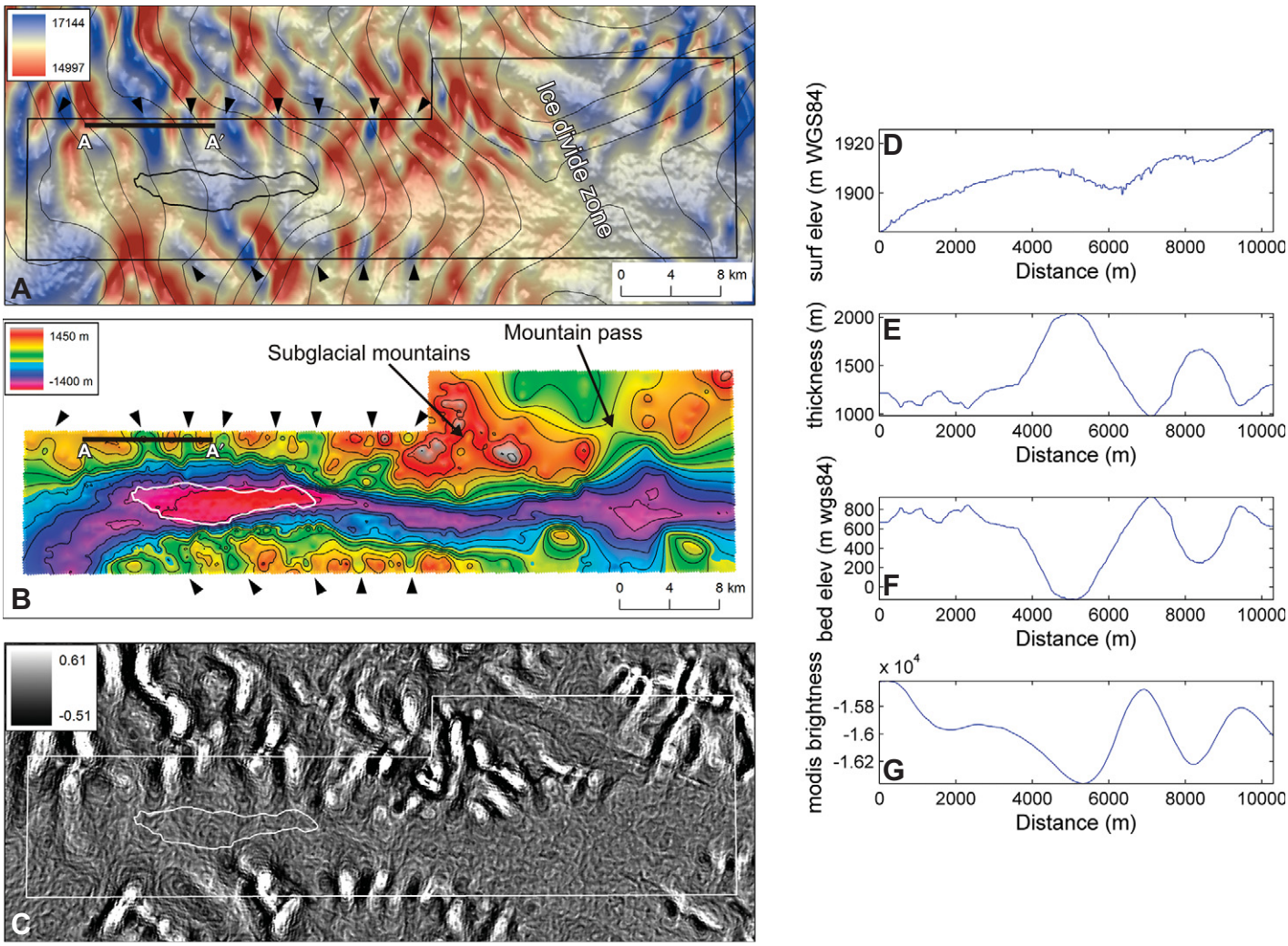

Figure 5. (A) Moderate-Resolution Imaging Spectroradiometer (MODIS) Mosaic of Antarctica (MOA) ice-surface imagery of the northwestern parts of Ellsworth Trough (Ellsworth Subglacial Lake and its locale) draped over a hillshade image of the same data. Black arrows indicate the positions of hanging tributary valleys identified in bed topography data. Thin black outline (reproduced as white outlines in panels B and C) is area of Ellsworth Subglacial Lake; thick black line (also shown in panel B) is location of radio-echo sounding (RES) survey line C9 (see Fig. 4). Ice-surface contours (thin black lines), at 10 m intervals, are derived from the 1 km ice surface digital elevation model of Bamber et al. (2009b). Black box is area of bed topography data in part B. (B) Subglacial bed topography around Ellsworth Subglacial Lake derived from ground-based RES data. Contours are in 200 m intervals. (C) Profile curvature of the MODIS MOA imagery. (D) Ice-surface elevation of survey line C9. (E) Ice thickness of survey line C9. (F) Bed elevation of survey line C9. (G) Values of MODIS ice-surface imagery extracted along survey line C9.

orthogonally oriented hanging tributary valleys, are present throughout the entire Ellsworth Subglacial Highlands (Fig. 6C). A series of major troughs lie between the western flank of the Sentinel Range and the Ellsworth Trough. Some of these troughs, highlighted previously by King (2009), drain Ellsworth Mountains ice northward into the Rutford Ice stream and have clear trough heads (Linton, 1963). From the MODIS imagery, we recognize a series of other, previously unreported or little documented troughs within the Ellsworth Subglacial Highlands (Fig. 6C). Our analysis suggests that at least three further troughs (T1, T3, T4, and possibly T5) may breach the entire Ellsworth Subglacial Highlands massif in a manner similar to the Ellsworth Trough (Fig. 6C). A very narrow trough, which reaches a depth of 1295 m bsl (see seismic station 630 of the Sentinel Mountains Traverse of Bentley and Ostenso, 1961), is located between the Ellsworth Trough and the Heritage Range of the Ellsworth Mountains (Figs. 2 and 6C), and it truncates the cirque-headed valleys that adorn the western flanks of these mountains. The MODIS MOA data suggest that this narrow trough likely connects directly with T1 in Figure 3C. Two further troughs (T3 and T4) are located further west than the Ellsworth Trough, on either side of the Martin–Nash Hills subglacial massif (Drewry and Jordan, 1983; Garrett et al., 1988; Ross et al., 2012; Jordan et al., 2013) (Fig. 7). T3 is a major trough incised deeply between the Whitmore Mountains and Mounts Woollard and Moore (Drewry and Jordan, 1983; Garrett et al., 1988). T3, T4, the Ellsworth Trough, and a sixth large trough (T5) are associated with zones of ice-surface "drawdown," manifested as a series of ice-surface "saddles" along the axis of the Amundsen-Weddell and Weddell-Ross

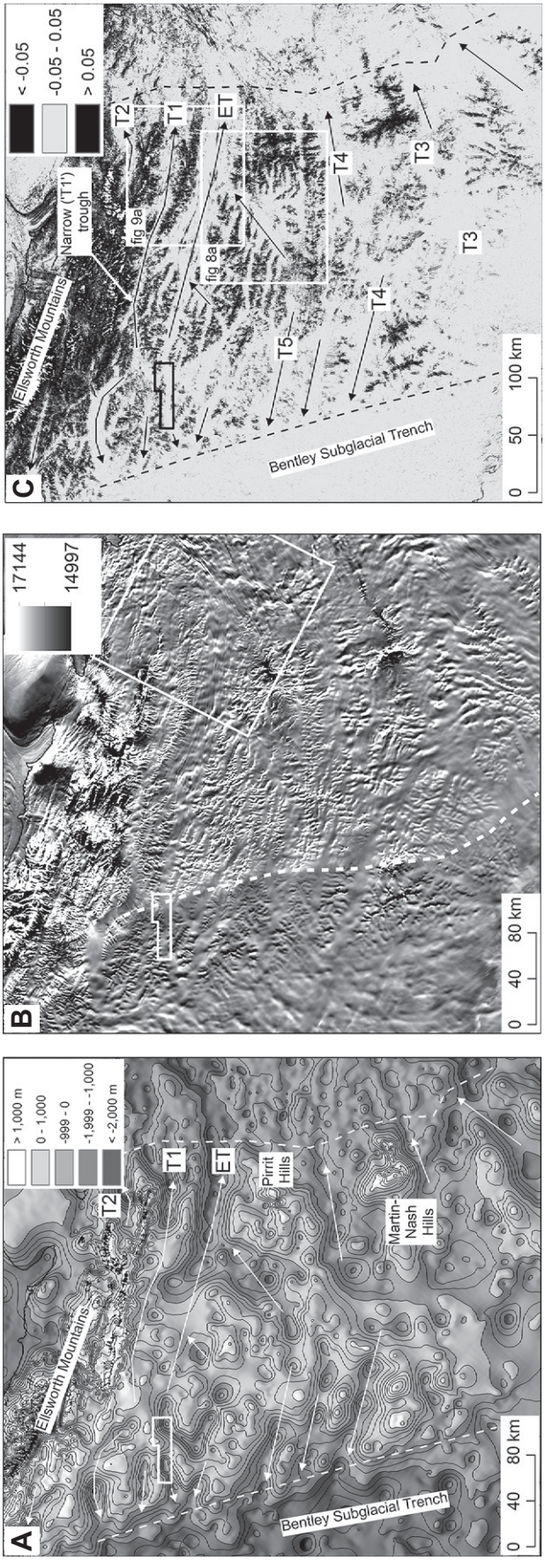

Figure 6. (A) Subglacial topography of the Ellsworth Subglacial Highlands (BEDMAP2) (Fretwell et al., 2013). White arrows show the broad paleo–ice-field ice-flow regime inferred from the ice-surface imagery and the subglacial topography data. Dashed white lines show the inferred ice-field limit. ET—Ellsworth Trough. (B) Moderate-Resolution Imaging Spectroradiometer (MODIS) Mosaic of Antarctica (MOA) ice-surface imagery (Haran et al., 2005). White dashed line shows approximate position of present-day ice divide. Small white box shows the extent of the radio-echo sounding (RES) survey around Ellsworth Subglacial Lake. Large white box is the area of Figure 3C. (C) Profile curvature analysis map of MODIS MOA ice-surface data. Black arrows show the broad ice-field ice-flow regime inferred from the ice-surface imagery and the subglacial topography data. Dashed black lines show the inferred ice-field limit. White boxes show extent of Figures 8A and 9A; Figures 6A, 6B, and 6C have the same extent as Figures 1B and 7A.

sections of the primary West Antarctic Ice Sheet divide (Fig. 7A). MODIS MOA imagery reveals significant geomorphic detail, not apparent from along-track RES data, demonstrating that these major troughs are associated with a complex of dendritic, transection tributary valleys, particularly to the south of the nunataks of Mount Woollard and Mount Moore (Fig. 7B).

Careful examination of MODIS MOA imagery elsewhere across the Ellsworth Subglacial Highlands reveals similarly detailed glacial geomorphic information additional to that revealed by RES data. The Pirrit Hills are the subaerial representation of a large subglacial massif that lies to the west of the Ellsworth Trough beneath the Institute ice stream catchment (Fig. 8). Radar data show that the Pirrit Hills massif, which is predominantly composed of Jurassic granite (Storey et al., 1988; Jordan et al., 2013), has been highly dissected by glacial erosion (Fig. 8B). To the north of the subglacial massif, beyond the high-resolution, gridded part of our aerogeophysical survey (Figs. 1 and 3), the MODIS imagery reveals a subglacial valley complex, consisting of a deep central basin and a series of radial tributary valleys (Fig. 8A). The central basin hosts a limb of the present-day Ellsworth Trough enhanced-flow tributary of the Institute ice stream (Fig. 8A). The planform of the valley complex is dendritic, reflecting a preglacial period of fluvially dominated landscape evolution. During later periods of restricted glaciation, however, (i.e., when the Ellsworth Subglacial Highlands supported an ice cap or ice field), these valleys would play an important role in controlling the direction of ice flow, draining ice into the southeastern part of the Ellsworth Trough.

Across the Ellsworth Trough from the Pirrit Hills, to the northeast of the trough and the enhanced-flow tributary of the Institute ice stream (Fig. 2C), we identify a series of ice-surface features, orthogonal to present-day ice flow, on the northeastern flanks of the trough (Fig. 9A). The MODIS MOA imagery reveals these features to be a complex of near-ice-surface subglacial hanging valleys, separated by prominent spurs and arêtes, adorning a 100-km-long, linear subglacial mountain ridge composed of a mixture of Cambrian–Permian metasediments and Cambrian volcanics (Jordan et al., 2013; Fig. 9). The form and spacing of these landforms are directly comparable to subaerial hanging valleys and spurs observed on the western flanks of the Sentinel Range, reinforcing our interpretation that the ice-surface features we observe and identify from the MODIS MOA, and from the profile curvature analysis of the MODIS mosaic, are representative of the subglacial geomorphology beneath.

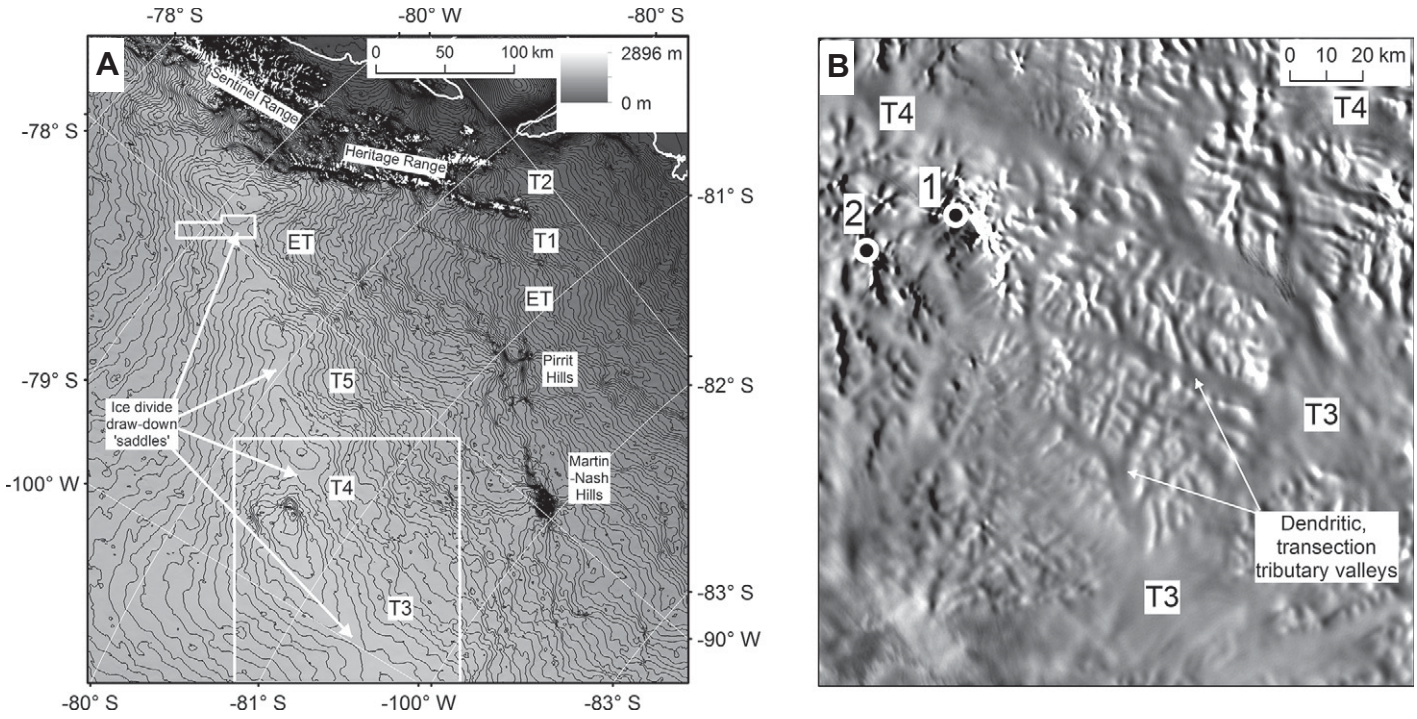

Figure 7. (A) Ice-sheet surface elevation over the Ellsworth Subglacial Highlands derived from GLAS/ICESat 500 m laser altimetry digital elevation model of Antarctica (DiMarzio et al., 2007) (extent of Fig. 7A is the same as Figs. 6A–6C and 1B). Contours are in 20 m intervals. Large white box shows extent of part B; small white box shows extent of ground-based radio-echo sounding (RES) around Ellsworth Subglacial Lake. ET—Ellsworth Trough. (B) Moderate-Resolution Imaging Spectroradiometer (MODIS) Mosaic of Antarctica (MOA) surface morphology imagery (Haran et al., 2005) of the area to the south of Mount Moore (1) and Mount Woollard (2) showing dendritic network of transection valleys. Note correspondence between drawn-down parts of the ice divide in A and the smooth areas of the optical imagery, believed to represent deep subglacial troughs, in B.

ELLSWORTH SUBGLACIAL HIGHLAND ICE FIELD

At its maximum, the Ellsworth Trough is ~325 km long and more than 25 km wide (Fig. 2), comparable in scale and dimensions to the troughs beneath Byrd Glacier and Beardmore Glacier in East Antarctica (Stearns et al., 2008; Denton et al., 1989), and Jakobshavn Isbrae in western Greenland (Peters et al., 2012). Understanding the geomorphology of the Ellsworth Trough is key to reconstructing the configuration of the paleo–ice mass(es) responsible for its formation.

The subglacial landforms associated with the Ellsworth Trough (hanging tributary valleys, valley steps, valley overdeepenings rising to prominent ridges, and down-ice-flow valley widening) are consistent with the geomorphology of a glacially carved fjord (e.g., Holtedahl, 1967). The ridges are particularly indicative; bedrock ridges often form in fjord-mouths because of a sudden decrease in the erosive capacity. This decrease is due to: (1) a shift to a divergent ice-flow regime, caused by the sudden lack of lateral constraint from valley sidewalls at the valley mouth (Holtedahl, 1967; Shoemaker 1986); and (2) the glacier approaching flotation near its tidewater-terminating margin (Crary, 1966). The reduction in basal erosion rates leads to an abrupt termination to the valley overdeepening and the formation of the threshold. The ridges identified at both the northwestern and southeastern ends of the Ellsworth Trough (Ellsworth Subglacial Lake Ridge and R2) are located across the entire width of the valley at the down-ice end of significant overdeepenings at points where the valley widens down-ice and are therefore interpreted as fjord-mouth threshold bars (Fig. 3). The location of overdeepenings immediately down-ice of tributary valley confluences (e.g., in the northwestern part of the Ellsworth Trough) is consistent with normal fjord geometry and a convergent ice-flow regime (Crabtree, 1981), while subglacial erosion by meltwater, such as might be represented by a possible channel incised into the northwestern threshold bar (Ellsworth Subglacial Lake Ridge), is also well documented within fjords (Holtedahl, 1967). Hence, the Ellsworth Trough represents evidence of former highly erosive dynamic glaciers terminating into water at valley mouths.

The overdeepenings (at least one of which is asymmetric in profile) with threshold bars at both ends of the Ellsworth Trough suggest that the trough was cut by an ice mass centered over the Ellsworth Subglacial Highlands, rather than by the advancing margin of an ice sheet impeded by the rock barrier of the Ellsworth Subglacial Highlands. As such, the broad-scale mechanism for the formation of the Ellsworth Trough is different from that proposed for large troughs in East Antarctica (Young et al., 2011) and the Transantarctic Mountains (Sugden and Denton, 2004), although the primary process (glacial erosion) is the same. Instead, trough incision took place when restricted ice masses occupied the Ellsworth Subglacial Highlands. We reject the idea that the overdeepenings and threshold bars were formed beneath present-day ice-sheet conditions; the rate of ice flow over the vast majority of the Ellsworth Subglacial Highlands, in the interior of the ice sheet, is slow (<25 m yr^{-1}) (Ross et al., 2011; Rignot et al., 2011), prohibiting significant recent basal erosion. Furthermore, the formation of the landform assemblage surrounding the trough (i.e., rugged mountainous topography with hanging tributary valleys) is entirely incompatible with the

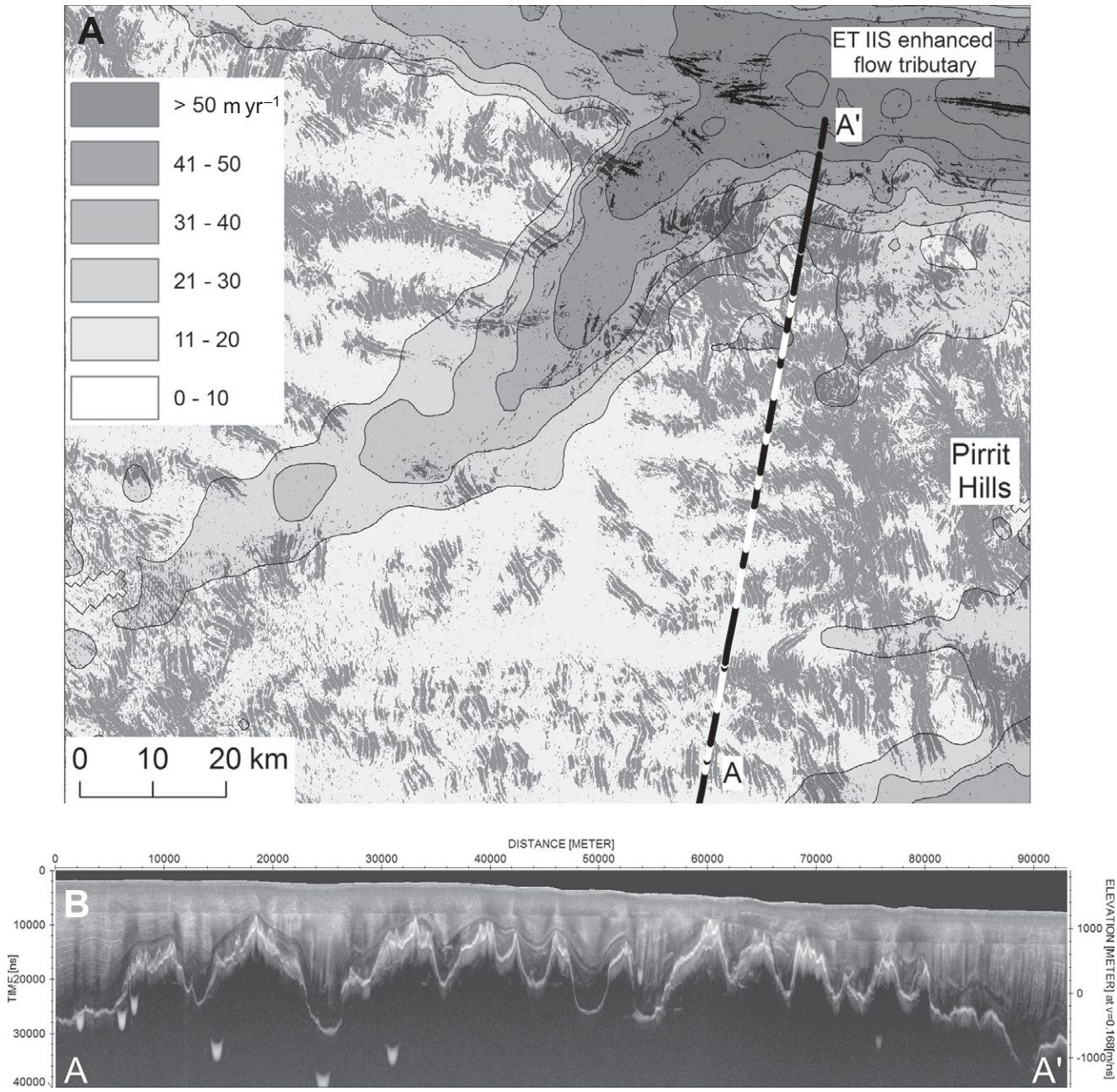

Figure 8. (A) Profile curvature analysis map of Moderate-Resolution Imaging Spectroradiometer (MODIS) Mosaic of Antarctica (MOA) ice-surface data with ice-sheet surface velocity map (Rignot et al., 2011) superimposed. Cells with curvature <–0.05 and >0.05 are colored black; cells with curvature between –0.05 and 0.05 are colored light gray. Line A-A′ shows survey line of radargram in B. Black sections of line show topography <250 m above sea level (asl; i.e., deep valleys); white sections show topography >250 m asl (i.e., subglacial highlands). The profile curvature map clearly reflects the subglacial topography beneath. IIS—Institute ice stream. (B) Radargram (A-A′) showing subglacial topography of the northern side of the Pirrit Hills. The ice flow that cut these U-shaped valleys is inferred to have been into the radargram, from the Pirrit Hills toward the broad basin that feeds the Ellsworth Trough (ET).

present-day cold-based regime of the thinner parts of the ice sheet; deep, U-shaped hanging tributary valleys incised to elevations around present-day sea level (e.g., Fig. 4) require warm-based conditions for their formation.

Glacial troughs and fjords breaching massifs along structural weaknesses and sometimes across preexisting fluvial valleys have long been recognized as diagnostic features of glacial erosion by ice sheets (e.g., in Scotland, North America, Norway, Greenland, and Chile; Holtedahl, 1967; Sugden 1968, 1974, 1978; Nesje and Whillans, 1994; Glasser and Ghiglione, 2009). The northwest to southeast orientation of the Ellsworth Trough, and other immediately adjacent subglacial troughs, parallels the dominant structural grain of the Ellsworth Mountains, where fold axial planes in Cambrian–Permian metasediments are aligned northwest to southeast (Craddock et al., 1992; Spörli and Craddock, 1992; Curtis, 2001). Prominent mag-

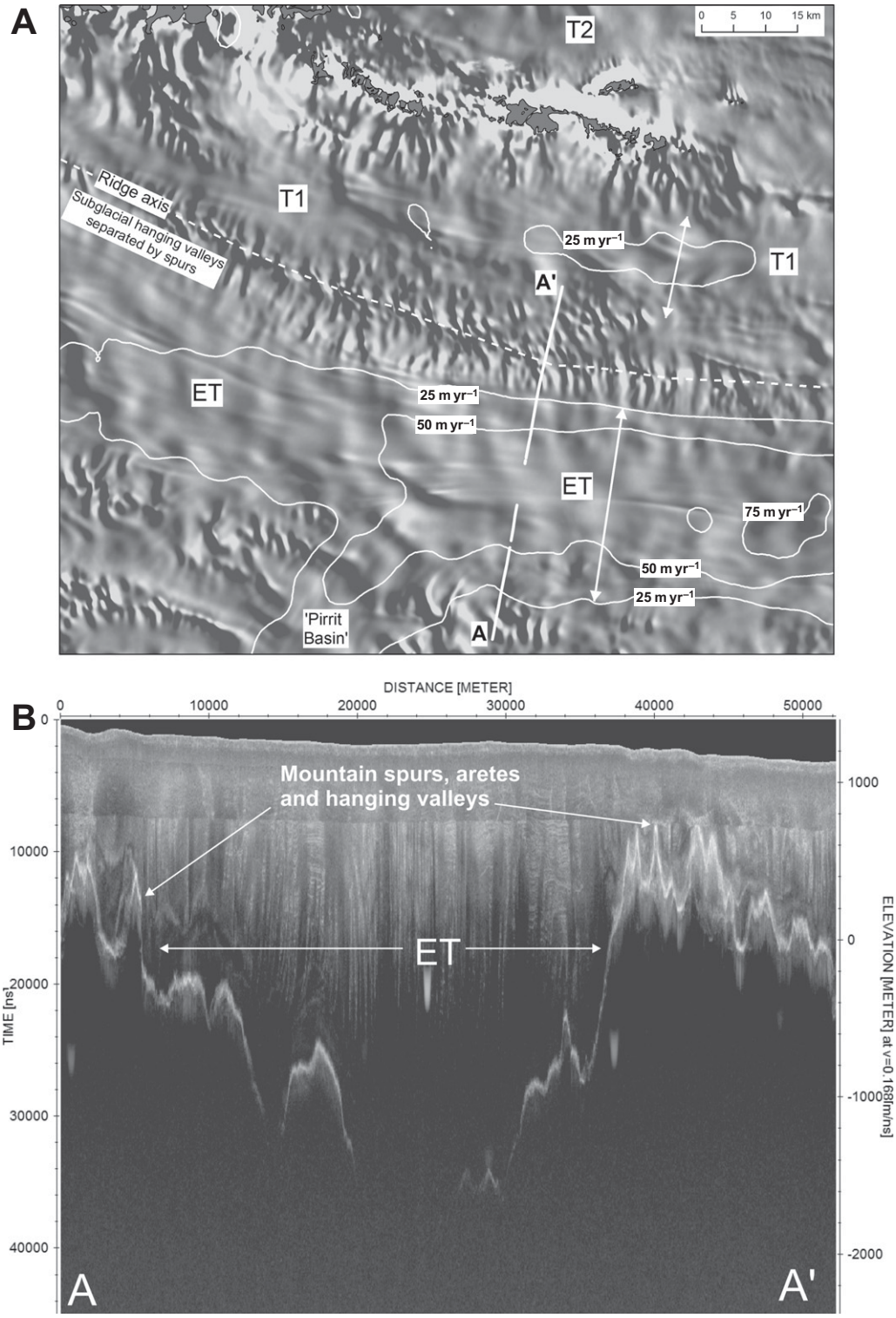

Figure 9. (A) Moderate-Resolution Imaging Spectroradiometer (MODIS) Mosaic of Antarctica (MOA) ice-surface imagery of an ~100-km-long subglacial mountain ridge that separates the Ellsworth Trough (ET) from the adjacent valley T1 ("narrow" trough). The mountain ridge is adorned with a series of subglacial hanging valleys, separated by arêtes, which are tributaries of these troughs. The Ellsworth Trough hosts an enhanced-flow tributary of the Institute ice stream. Contours (at 25 m intervals) of present-day ice surface velocities (Rignot et al., 2011), are superimposed to demonstrate the importance of these geomorphic features in controlling present-day ice flow. Grey filled polygons represent areas of exposed bedrock (from Antarctic Digital Database (ADD)). Broad white line (A-A′) across trough and adjacent ridges marks the location of radargram in 9b. Present-day ice flow along the troughs (Ellsworth Trough, T1 and T2) is approximately left to right; (B) Radargram showing the deep Ellsworth Trough (ET) bounded by mountainous subglacial topography with hanging valleys, arêtes, and mountain spurs. Present-day ice flow is approximately out of page. Note that the bed is not sounded in the deepest parts of the trough, which in this radargram represents bed below ~1600 m below sea level (section without data is represented by the break in line A-A′ in 9a).

netic lineaments over the Ellsworth Mountains have also recently been interpreted as revealing NW-SE–oriented basement faults (Jordan et al., 2013). The Ellsworth Trough and the other Ellsworth Subglacial Highlands troughs are therefore likely to have been formed by an ice mass exploiting and eroding these preexisting structural weaknesses (i.e., through "selective linear erosion"; cf. Bingham et al., 2012).

The form of the Ellsworth Trough, the prominent overdeepenings, and the hanging valleys are all diagnostic of a dynamic alpine glaciated valley environment associated with a predominantly maritime climate. The troughs must have formed when the marine sections of the West Antarctic Ice Sheet were largely absent (either prior to West Antarctic Ice Sheet development or during a "collapse" event), when small ice fields occupied the topographic highlands of the region, confirming previous hypotheses about West Antarctic Ice Sheet initiation and

decay (Bentley et al., 1960; Bamber et al., 2009; DeConto and Pollard, 2003). On such occasions, with global ice volumes below present-day levels and without West Antarctic isostatic depression, the present-day Bentley Subglacial Trench would have been a deep marine basin, with a coastline along the edge of the present-day Ellsworth Subglacial Highlands. To the southeast, the deep marine basins underlying Institute ice stream and Möller Ice stream (Janowski and Drewry, 1981; Ross et al., 2012) would also have been inundated. The former glacier within the Ellsworth Trough is therefore likely to have terminated as a tidewater glacier, consistent with our interpretation of the bedrock ridges identified in RES data as fjord-mouth threshold bars, and the margin of the associated grounded ice field well defined at the flanks of the Ellsworth Subglacial Highlands. The asymmetry of the overdeepenings (Fig. 3) and the planform of the tributary complex northwest of the Pirrit Hills (Fig. 8A) suggest that the flow of this ice field was separated by a primary divide located over the axis of the Ellsworth Subglacial Highlands, near to, and with a similar orientation to, the present-day Amundsen-Weddell divide (Fig. 7) (Ross et al., 2011).

We have no direct dates on the landforms of the Ellsworth Subglacial Highlands, so we cannot determine a robust age for trough formation and the dissection of the Ellsworth Subglacial Highlands. The landscape is clearly a composite one, however, having formed during a series of alpine glaciations over the last 34 m.y. through a combination of glacial and subaerial (erosion) processes when the marine ice sheet was absent. Subglacial evidence (Scherer et al., 1998) and far-field sea-level data (e.g., Raymo and Mitrovica, 2012) support a restricted West Antarctic Ice Sheet during marine isotope stage 11 (420–360 ka), but the duration of this interglacial (<60 k.y.) was too short to allow the incision of >1-km-deep troughs into the predominantly metasedimentary bedrock of the Ellsworth Subglacial Highlands at that time (Kessler et al., 2008). Instead, it is likely that the most recent significant erosion of the Ellsworth Subglacial Highlands occurred during the early Pliocene (4.6–3.3 Ma), when the marine sections of the West Antarctic Ice Sheet were significantly diminished (McKay et al., 2012).

Unlike major former ice-sheet changes in East Antarctica, which would require substantial alteration to climate and ocean conditions to occur (e.g., Bo et al., 2009), restricted ice caps in West Antarctica may well be consistent with the present climate if the current ice mass were to decay. For example, the Antarctic Peninsula, to the immediate north of the Ellsworth Subglacial Highlands, currently contains several modest-sized ice caps (e.g., Dyer Plateau, Avery Plateau) that cover subglacial highlands and terminate in water. Deep fjord structures, which have overdeepened basins and steps, and which follow geological structure, underlie, or have underlain, the outlet glaciers of these ice caps (Crabtree, 1981; Scambos et al., 2011).

CONCLUSIONS

We have: (1) characterized the detailed subglacial morphology (U-shaped troughs, hanging tributary valleys, valley overdeepenings, and threshold sills) of the Ellsworth Subglacial Highlands, West Antarctica; (2) identified and mapped a series of deep subglacial troughs, one of which, the Ellsworth Trough, is >25 km across and >300 km long, and is incised into, and breaches, the Ellsworth Subglacial Highlands; (3) reconstructed the glaciology and flow regime of the ice mass responsible for the form of the Ellsworth Subglacial Highlands, to show that the subglacial landscape was cut by a small, dynamic, highly erosive, warm-based, marine-proximal ice field, characterized by tidewater (fjord-mouth) margins; and (4) demonstrated the considerable potential provided by the application and analysis of satellite remote-sensing imagery of the ice-sheet surface for the mapping of subglacial topography.

Our findings support the proposition that, in the absence of a large-scale marine ice sheet, small dynamic ice caps or ice fields characterized, at least in part, by tidewater margins, are likely to be centered on the prominent highlands in West Antarctica (Bentley et al., 1960; DeConto and Pollard, 2003; Pollard and DeConto, 2009). These ice masses, similar in character and dynamics to those of the present-day Antarctic Peninsula, play a key role in the seeding and early growth of the marine-based sectors of the West Antarctic Ice Sheet and in the stabilization of retreating marine-based West Antarctic Ice Sheets (Bentley et al., 1960; Weertman, 1974; Bamber et al., 2009).

ACKNOWLEDGMENTS

Financial support was provided by the UK Natural Environment Research Council (NERC) Antarctic Funding Initiative (AFI) grants NE/G013071/1 and NE/D008638/1. The NERC Geophysical Equipment Facility provided GPS equipment (loans 838, 870). We thank the British Antarctic Survey for logistics support, J. Woodward, A. Smith, E. King, R. Hindmarsh, and D. Vaughan for assistance in the planning and acquisition of DELORES data from Lake Ellsworth, M. Bentley and D. Sugden for discussion of an earlier draft of this manuscript, A. Rivera for sharing unpublished radar data, and M. LeCompte for advice on remote-sensing imagery. D. Fitzgerald, D. Routledge, C. Robinson, I. Potten, D. Cochrane, and M. Oostlander are thanked for their invaluable support in the field. Two reviewers and the associate editor are thanked for insightful comments that significantly improved the manuscript. We would also like to acknowledge the hard work done by the Moderate-Resolution Imaging Spectroradiometer (MODIS) Mosaic of Antarctica (MOA) team in compiling the MOA imagery. Without it, this work would not have been possible.

REFERENCES CITED

Bamber, J.L., Riva, R.E.M., Vermeersen, B.L.A., and LeBrocq, A.M., 2009a, Reassessment of the potential sea-level rise from a collapse of the West Antarctic Ice Sheet: Science, v. 324, p. 901–903, doi:10.1126/science.1169335.

Bamber, J.L., Gomez-Dans, J.L., and Griggs, J.A., 2009b, Antarctic 1 km Digital Elevation Model (DEM) from Combined ERS-1 Radar and ICESat Laser Satellite Altimetry: Boulder, Colorado, National Snow and Ice Data Center (digital media).

Bell, R.E., Ferraccioli, F., Creyts, T.T., Braaten, D., Corr, H., Das, I., Damaske, D., Frearson, N., Jordan, T., Rose, K., Studinger, M., and Wolovick, M., 2011, Widespread persistent thickening of the East Antarctic Ice Sheet by freezing from the base: Science, v. 331, p. 1592–1595, doi:10.1126/science.1200109.

Bentley, C., and Ostenso, N.A., 1961, Glacial and subglacial topography of West Antarctica: Journal of Glaciology, v. 29, p. 882–912.

Bentley, C.R., Crary, A.P., Ostenso, N.A., and Thiel, E.C., 1960, Structure of West Antarctica: Science, v. 131, p. 131–136, doi:10.1126/science.131.3394.131.

Bentley, M.J., 2010, The Antarctic palaeo-record and its role in improving predictions of future Antarctic Ice Sheet change: Journal of Quaternary Science, v. 25, p. 5–18, doi:10.1002/jqs.1287.

Bingham, R.G., Ferraccioli, F., King, E.C., Larter, R.D., Pritchard, H.D., Smith, A.M., and Vaughan, D.G., 2012, Inland thinning of West Antarctic Ice Sheet steered along subglacial rifts: Nature, v. 487, p. 468–471, doi:10.1038/nature11292.

Blankenship, D.D., Morse, D.L., Finn, C.A., Bell, R.E., Peters, M.E., Kempf, S.E., Hodge, S.M., Studinger, M., Behrendt, J.C., and Brozena, J.M., 2001, Geologic controls on the initiation of rapid basal motion for the West Antarctic ice streams: A geophysical perspective including new airborne radar sounding and laser altimetry results, *in* Alley, R.B., and Bindschadler, R.A., eds., The West Antarctic Ice Sheet: Behavior and Environment: Washington, D.C., American Geophysical Union, Antarctic Research Series 77, p. 283–296.

Bo, S., Siegert, M.J., Mudd, S.M., Sugden, D., Fujita, S., Xiangbin, C., Younyou, J., Xueyuan, T., and Yuansheng, L., 2009, The Gamburtsev Mountains and the origin and early evolution of the Antarctic Ice Sheet: Nature, v. 459, p. 690–693, doi:10.1038/nature08024.

Corr, H., Ferraccioli, F., Frearson, N., Jordan, T., Robinson, C., Armadillo, E., Caneva, G., Bozzo, E., and Tabacco, I., 2007, Airborne radio-echo sounding of the Wilkes Subglacial Basin, the Transantarctic Mountains, and the Dome C region: Terra Antartica Reports, v. 13, p. 55–64.

Crabtree, R.D., 1981, Subglacial morphology in northern Palmer Land, Antarctic Peninsula: Annals of Glaciology, v. 2, p. 17–22, doi:10.3189/172756481794352496.

Craddock, C., Spörli, K.B., and Anderson, J.J., 1992, Structure of the Sentinel Range, Ellsworth Mountains, West Antarctica, *in* Webers, G.F., Craddock, C., and Splettstoesser, J.F., eds., Geology and Paleontology of the Ellsworth Mountains, West Antarctica: Geological Society of America Memoir 170, p. 393–402.

Crary, A.P., 1966, Mechanism for fiord formation indicated by studies of an ice-covered inlet: Geological Society of America Bulletin, v. 77, p. 911–930.

Curtis, M.L., 2001, Tectonic history of the Ellsworth Mountains, West Antarctica: Reconciling a Gondwana enigma: Geological Society of America Bulletin, v. 113, p. 939–958.

DeConto, R.M., and Pollard, D., 2003, Rapid Cenozoic glaciation of Antarctica induced by declining atmospheric CO_2: Nature, v. 421, p. 245–249, doi:10.1038/nature01290.

Denton, G.H., Bockheim, J.G., Wilson, S.C., Leide, J.E., and Andersen, B.G., 1989, Late Quaternary ice-surface fluc-

tuations of Beardmore Glacier, Transantarctic Mountains: Quaternary Research, v. 31, p. 183–209, doi: 10.1016/0033-5894(89)90005-7.

Denton, G.H., Bockheim, J.G., Rutford, R.H., and Andersen, B.G., 1992, Glacial history of the Ellsworth Mountains, West Antarctica, *in* Webers, G.F., Craddock, C., and Splettstoesser, J.F., eds., Geology and Palaeontology of the Ellsworth Mountains, West Antarctica: Geological Society of America Memoir 170, p. 403–432.

DiMarzio, J., Brenner, A., Fricker, H., Schutz, R., Shuman, C.A., and Zwally, H.J., 2007, GLAS/ICESat 500 m Laser Altimetry Digital Elevation Model of Antarctica: Boulder, Colorado, National Snow and Ice Data Center (digital media).

Drewry, D.J., and Jordan, S.R., 1983, The bedrock surface of Antarctica, *in* Antarctica: Glaciological and Geophysical Folio: Cambridge, UK, Scott Polar Research Institute.

Ferraccioli, F., Finn, C.A.. Jordan, T.A., Bell, R.E., Anderson, L.M., and Damaske, D., 2011, East Antarctic rifting triggers uplift of the Gamburtsey Mountains: Nature, v. 479, p. 388–394.

Fretwell, P., Pritchard, H.D., Vaughan, D.G., Bamber, J.L., Barrand, N.E., Bell, R., Bianchi, C., Bingham, R.G., Blankenship, D.D., Casassa, G., Catania, G., Callens, D., Conway, H., Cook, A.J., Corr, H.F.J., Damaske, D., Damm, V., Ferraccioli, F., Forsberg, R., Fujita, S., Gim, Y., Gogineni, P., Griggs, J.A., Hindmarsh, R.C.A., Holmlund, P., Holt, J.W., Jacobel, R.W., Jenkins, A., Jokat, W., Jordan, T., King, E.C., Kohler, J., Krabill, W., Riger-Kusk, M., Langley, K.A., Leitchenkov, G., Leuschen, C., Luyendyk, B.P., Matsuoka, K., Mouginot, J., Nitsche, F.O., Nogi, Y., Nost, O.A., Popov, S.V., Rignot, E., Rippen, D.M., Rivera, A., Roberts, J., Ross, N., Siegert, M.J., Smith, A.M., Steinhage, D., Studinger, M., Sun, B., Tinto, B.K., Welch, B.C., Wilson, D., Young, D.A., Xiangbin, C., Zirizzotti, A., 2013, Bedmap2: Improved ice bed, surface and thickness datasets for Antarctica: The Cryosphere, v. 7, p. 375–393.

Garrett, S.W., Maslanyi, M.P., and Damaske, D., 1988, Interpretation of aeromagnetic data from the Ellsworth Mountains-Thiel ridge, West Antarctica: Journal of the Geological Society, London, v. 145, p. 1009–1017.

Glasser, N.F., and Ghiglione, M.C., 2009, Structural, tectonic and glaciological controls on the evolution of fjord landscapes: Geomorphology, v. 105, p. 291–302, doi:10.1016/j.geomorph.2008.10.007.

Gudmundsson, G.H., 2003, Transmission of basal variability to a glacier surface: Journal of Geophysical Research, v. 108, p. 2253, doi:10.1029/2002JB002107.

Haran, T., Bohlander, J., Scambos, T., Painter, T., and Fahnestock, M., 2005 (updated 2006), MODIS Mosaic of Antarctica (MOA) Image Map: Boulder, Colorado, National Snow and Ice Data Center (digital media).

Holtedahl, H., 1967, Notes on the formation of fjords and fjord-valleys: Geografiska Annaler, ser. A, Physical Geography, v. 49, p. 188–203, doi:10.2307/520887.

Janowski, E.J. and Drewry, D.J., 1981, The structure of West Antarctica from geophysical studies: Nature, v. 291, p. 17–21.

Jezek, K.C., 1999, Glaciological properties of the Antarctic ice sheet from RADARSAT-1 synthetic aperture radar imagery: Annals of Glaciology, v. 29, p. 286–290, doi:10.3189/172756499781820969.

Jordan, T.A., Ferraccioli, F., Ross, N., Siegert, M.J., Corr, H.F.J., Leat, P.T., Bingham, R.G., Rippin, D.M., and Le Brocq, A., 2013, Inland extent of the Weddell Sea rift imaged by new aerogeophysical data: Tectonophysics, v. 585, p. 137–160, doi:10.1016/j.tecto.2012.09.010.

Joughin, I., and Alley, R.B., 2011, Stability of the West Antarctic Ice Sheet in a warming world: Nature Geoscience, v. 4, p. 506–513, doi:10.1038/ngeo1194.

Joughin, I., Bamber, J.L., Scambos, T., Tulaczyk, S., Fahnestock, M., and MacAyeal, D.R., 2006, Integrating satellite observations with modelling: Basal shear stress of the Filchner-Ronne ice streams, Antarctica: Philosophical Transactions of the Royal Society, ser. A, v. 364, p. 1795–1814, doi:10.1098/rsta.2006.1799.

Karlsson, N.B., Rippin, D.M., Bingham, R.G., and Vaughan, D.G., 2012, Determination of a "continuity-index" for assessing ice-sheet dynamics from radar-sounded internal layers: Earth and Planetary Science Letters, v. 335–336, p. 88–94, doi:10.1016/j.epsl.2012.04.034.

Kessler, M.A., Anderson, R.S., and Briner, J.P., 2008, Fjord insertion into continental margins driven by topographic steering of ice: Nature Geoscience, v. 1, p. 365–369, doi:10.1038/ngeo201.

Kimerling, A.J., Buckley, A.R., Muehrcke, P.C., and Muehrcke, J.O., 2011, Map Use: Reading Analysis Interpretation: ESRI Press, 620 p.

King, E.C., 2009, Flow dynamics of the Rutford ice stream ice-drainage basin, West Antarctica, from radar stratigraphy: Annals of Glaciology, v. 50, p. 42–48, doi:10.3189/172756409789097586.

Le Brocq, A.M., Hubbard, A., Bentley, M.J., and Bamber, J.L., 2008, Subglacial topography inferred from ice surface terrain analysis reveals a large un-surveyed basin below sea level in East Antarctica: Geophysical Research Letters, v. 35, L16503, doi:10.1029/2008GL034728.

Linton, D.L., 1963, The forms of glacial erosion: Transactions of the Institute of British Geographers, v. 33, p. 1–28.

McKay, R., Naish, T., Carter, L., Riesselman, C., Dunbar, R., Sjunneskog, C., Winter, D., Sagiorgi, F., Warren, C., Pagani, M., Schouten, S., Willmott, V., Levy, R., DeConto, R., and Powell, R.D., 2012, Antarctic and Southern Ocean influences on late Pliocene global cooling: Proceedings of the National Academy of Sciences of the United States of America, v. 109, p. 6423–6428, doi:10.1073/pnas.1112248109.

Nesje, A., and Whillans, I.M., 1994, Erosion of Sognefjord, Norway: Geomorphology, v. 9, p. 33–45, doi:10.1016/0169-555X(94)90029-9.

Peters, L.E., Anandakrishnan, S., Alley, R.B., and Voight, D.E., 2012, Seismic attenuation in glacial ice: A proxy for englacial temperature: Journal of Geophysical Research, v. 117, F02008, doi:10.1029/2011JF002201.

Pollard, D., and DeConto, R.M., 2009, Modelling West Antarctic Ice Sheet growth and collapse through the past five million years: Nature, v. 458, p. 329–332, doi:10.1038/nature07809.

Raymo, M.E., and Mitrovica, J.X., 2012, Collapse of polar ice sheets during the stage 11 interglacial: Nature, v. 483, p. 453–456, doi:10.1038/nature10891.

Rémy, F., and Minster, J.-F., 1997, Antarctic ice sheet curvature and its relation with ice flow and boundary conditions: Geophysical Research Letters, v. 24, p. 1039–1042, doi:10.1029/97GL00959.

Rignot, E., Mouginot, J., and Scheuchl, B., 2011, Ice flow of the Antarctic ice sheet: Science, v. 333, p. 1427–1430, doi:10.1126/science.1208336.

Ross, N., Siegert, M.J., Woodward, J., Smith, A.M., Corr, H.F.J., Bentley, M.J., Hindmarsh, R.C.A., King, E.C., and Rivera, A., 2011, Holocene stability of the Amundsen-Weddell ice divide, West Antarctica: Geology, v. 39, p. 935–938, doi:10.1130/G31920.1.

Ross, N., Bingham, R.G., Corr, H.F.J., Ferraccioli, F., Jordan, T.A., Le Brocq, A., Rippin, D., Young, D., Blankenship, D., and Siegert, M.J., 2012, Weddell Sea sector of the West Antarctic Ice Sheet on the threshold of change: Nature Geoscience, v. 5, p. 393–396, doi:10.1038/ngeo1468.

Scambos, T.A., Haran, T.M., Fahnestock, M.A., Painter, T.H., and Bohlander, J., 2007, MODIS-based Mosaic of Antarctica (MOA) data sets: Continent wide surface morphology and snow grain size: Remote Sensing of Environment, v. 111, p. 242–257, doi:10.1016/j.rse.2006.12.020.

Scambos, T.A., Bethier, E., and Shuman, C.A., 2011, The triggering of subglacial lake drainage during rapid glacier drawdown: Crane Glacier, Antarctic Peninsula: Annals of Glaciology, v. 52, p. 74–82, doi:10.3189/172756411799096204.

Scherer, R.P., Aldahan, A., Tulaczyk, S., Kamb, B., Engelhardt, H., and Possnert, G., 1998, Pleistocene collapse of the West Antarctic Ice Sheet: Science, v. 281, p. 82–85, doi:10.1126/science.281.5373.82.

Shoemaker, E.M., 1986, The formation of fjord thresholds: Journal of Glaciology, v. 32, p. 65–71.

Siegert, M.J., Clarke, R.J., Mowlem, M., Ross, N., Hill, C.S., Tait, A., Hodgson, D., Parnell, J., Tranter, M., Pearce, D., Bentley, M.J., Cockell, C., Tsalogou, M.-N., Smith, A., Woodward, J., Brito, M.P., and Waugh, E., 2012, Clean access, measurement and sampling of Ellsworth Subglacial Lake: A method for exploring deep Antarctic subglacial lake environment: Reviews of Geophysics, v. 50, RG1003, doi:10.1029/2011RG000361.

Smith, B.E., Raymond, C.F., and Scambos, T., 2006, Anisotropic texture of ice sheet surfaces: Journal of Geophysical Research, v. 111, F01019, doi:10.1029/2005JF000393.

Spörli, K.B., and Craddock, C., 1992, Structure of the Heritage Range, Ellsworth Mountains, West Antarctica, *in* Webers, G.F., Craddock, C., and Splettstoesser, J.F., eds., Geology and Paleontology of the Ellsworth Mountains, West Antarctica: Geological Society of America Memoir 170, p. 375–392.

Stearns, L.A., Smith, B.E., and Hamilton, G.S., 2008, Increased flow speed on a large East Antarctic outlet glacier caused by subglacial floods: Nature Geoscience, v. 1, p. 827–831, doi:10.1038/ngeo356.

Storey, B.C., Hole, M.J., Pankhurst, R.J., Millar, I.L., and Vennum, W., 1988, Middle Jurassic within-plate granites in West Antarctica and their bearing on the break-up of Gondwanaland: Journal of the Geological Society of London, v. 145, p. 999–1007, doi:10.1144/gsjgs.145.6.0999.

Sugden, D.E., 1968, The selectivity of glacial erosion in the Cairngorms Mountains, Scotland: Transactions of the Institute of British Geographers, v. 45, p. 79–92, doi:10.2307/621394.

Sugden, D.E., 1974, Landscapes of glacial erosion in Greenland and their relationship to ice, topographic and bedrock conditions, *in* Waters, R.S., and Brown, E.H., eds., Progress in Geomorphology: Institute of British Geographers Special Publication 7, p. 177–195.

Sugden, D.E., 1978, Glacial erosion by the Laurentide ice sheet: Journal of Glaciology, v. 20, p. 367–391.

Sugden, D.E., and Denton, G., 2004, Cenozoic landscape evolution of the Convoy Range to Mackay Glacier area, Transantarctic Mountains: Onshore to offshore synthesis: Geological Society of America Bulletin, v. 116, p. 840–857, doi:10.1130/B25356.1.

Vaughan, D.G., Corr, H.F.J., Ferraccioli, F., Frearson, N., O'Hare, A., Mach, D., Holt, J.W., Blankenship, D.D., More, D.L., and Young, D.A., 2006, New boundary conditions for the West Antarctic Ice Sheet: Subglacial topography beneath Pine Island Glacier: Geophysical Research Letters, v. 33, L09501, doi:10.1029/2005GL025588.

Vaughan, D.G., Rivera, A., Woodward, J., Corr, H.F.J., Wendt, J., and Zamora, R., 2007, Topographic and hydrological controls on subglacial lake Ellsworth, West Antarctica: Geophysical Research Letters, v. 34, L18501, doi:10.1029/2007GL030769.

Weertman, J., 1974, Stability of the junction of an ice sheet and an ice shelf: Journal of Glaciology, v. 13, p. 3–11.

Welch, B.C., and Jacobel, R.W., 2005, Bedrock topography and wind erosion sites in East Antarctica: Observations from the 2002 US-ITASE traverse: Annals of Glaciology, v. 41, p. 92–96, doi:10.3189/172756405781813258.

Woodward, J., Smith, A.M., Ross, N., Thoma, M., Corr, H.F.J., King, E.C., King, M.A., Grosfeld, K., Tranter, M., and Siegert, M.J., 2010, Location for direct access to subglacial Lake Ellsworth: An assessment of geophysical data and modeling: Geophysical Research Letters, v. 37, L11501, doi:10.1029/2010GL042884.

Young, D.A., Wright, A.P., Roberts, J.L., Warner, R.C., Young, N.W., Greenbaum, J.S., Schroeder, D.M., Holt, J.W., Sugden, D.E., Blankenship, D.D., van Ommen, T.D., and Siegert, M.J., 2011, A dynamic early East Antarctic Ice Sheet suggested by ice-covered fjord landscapes: Nature, v. 474, p. 72–75, doi:10.1038/nature10114.

Science Editor: Christian Koeberl
Associate Editor: David R. Marchant

Manuscript Received 20 September 2012
Revised Manuscript Received 27 February 2013
Manuscript Accepted 1 March 2013

Printed in the USA